

Plasmonic and Nonlinear Optical Absorption Properties of Ag:ZrO₂ Nanocomposite Thin Films

Manish Kumar · C. S. Suchand Sandeep · G. Kumar ·
Y. K. Mishra · R. Philip · G. B. Reddy

Received: 27 April 2013 / Accepted: 18 July 2013 / Published online: 4 August 2013
© Springer Science+Business Media New York 2013

Abstract Ag nanoparticles (NPs) embedded in a zirconium oxide matrix in the form of Ag:ZrO₂ nanocomposite (NC) thin films were synthesized by using the sol–gel technique followed by thermal annealing. With the varying of the concentration of Ag precursor and annealing conditions, average sizes (diameters) of Ag nanoparticles (NPs) in the nanocomposite film have been varied from 7 to 20 nm. UV–VIS absorption studies reveal the surface plasmon resonance (SPR)-induced absorption in the visible region, and the SPR peak intensity increases with the increasing of the Ag precursor as well as with the annealing duration. A red shift in SPR peak position with the increase in the Ag precursor concentration confirms the growth of Ag NPs. Surface topographies of these NC films showed that deposited films are dense, uniform, and intact during the variation in annealing conditions. The magnitude and sign of absorptive nonlinearities were measured near the SPR of the Ag NPs with an open-aperture z-scan technique using a nanosecond-pulsed laser. Saturable optical absorption in NC films was identified having saturation intensities in the

order of 10¹² W/m². Such values of saturation intensities with the possibility of size-dependent tuning could enable these NC films to be used in nanophotonic applications.

Keywords Nanocomposites · Ag nanoparticles · Surface plasmon resonance · Nonlinear absorption

Introduction

Investigations on the plasmonic nanocomposites (NCs) comprising noble metal nanoparticles embedded in dielectric oxides are of paramount concern for variable linear and nonlinear optical (NLO) properties. Particularly, NLO properties are interesting owing to the possibility of fabricating photonic devices with superior performances. Strong NLO response of plasmonic NCs makes them suitable for devices of advanced telecommunication systems such as saturable optical absorbers and as optical limiters. Saturable optical absorbers in bistable optical devices provide optical switching or all optical memory functions; on the other hand, optical limiters can be used to prevent laser-induced damages [1, 2]. The ability of local field enhancement by noble metal nanostructures provides the prospects of the elaboration of ultrafast optical switches [3], optical limiters [4], reverse saturable absorbers [5], etc. The origin of nonlinear optical absorption due to local field enhancement by plasmons in metallo-dielectric NCs has been analyzed theoretically [6, 7] in detail, but only few relevant methods, e.g., Z-scan method [1, 2, 8, 9], can be used to experimentally investigate their NLO response.

These NCs show characteristic surface plasmon resonance (SPR) absorption in the visible region due to collective electron density oscillations at resonance frequencies [10, 11]. The peak position and the bandwidth of the plasmon absorption band depend on the size, shape, density distribution of nanoparticles, and also on the dielectric constant of the surrounding medium [12]. Altering postsynthesis external conditions (temperature,

M. Kumar · G. B. Reddy
Thin Film Laboratory, Department of Physics, Indian Institute
of Technology Delhi, New Delhi 110016, India

M. Kumar (✉)
Department of Physics, Central University of Rajasthan, Kishangarh,
Ajmer 305801, India
e-mail: manishbharadwaj@gmail.com

C. S. S. Sandeep · R. Philip
Light and Matter Physics Group, Raman Research Institute,
Sadashivanagar, Bangalore 560080, India

G. Kumar
Institute for Research in Electronics and Applied physics,
University of Maryland, College Park, MD 20742, USA

Y. K. Mishra
Institute for Materials Science, University of Kiel,
Kaiser Str. 2, 24143 Kiel, Germany

irradiation, etc.) cause changes in the effective dielectric constant of NCs which will significantly perturb the electron density oscillations, i.e., SPR absorption band in the NC film. This in turn affects the NLO behavior of the NC films because both the subpicosecond NLO response and thermomodulation are associated with the perturbation of the Fermi distribution of electrons in metal [13]. The shape- and size-dependent localized surface plasmon absorption effect in metallic nanoparticles makes them suitable candidates for applications viz. surface-enhanced Raman scattering, bimolecular detection, dielectric constant measurements, tailored plasmonic resonance, etc. [14–19]. The size dependence of the dielectric constant is determined by a free path effect [20, 21], which is based upon the Drude–Sommerfeld theory, and gives an expression for a size-dependent collision frequency of conduction electrons. The particle surface is considered as a scatterer of conduction electrons. The appropriate mean free path L_{sphere} of an electron, disregarding its coupling to the Fermi liquid, is calculated to be equal to the particle size (r). Provided that all scattering mechanisms of the conduction electrons in a spherical particle are independent of one another, the effective collision frequency ω_D is given by $\omega_D = \omega_{D, \text{bulk}} + v_F/r$, where v_F is Fermi velocity and $\omega_{D, \text{bulk}}$ is collision frequency of electrons in bulk metal. The local field enhancement inside nanoparticles is estimated with the field factor $f_1 = 3\varepsilon_m/(\varepsilon + 2\varepsilon_m)$, where ε and ε_m are dielectric constants of metal and embedding matrix, respectively [10, 13]. The nonlinearity of the composite is associated with the local field factor, absorbance, and the nonlinear susceptibilities, using arguments of effective medium approximations. The value of the third-order nonlinear susceptibility $\chi^{(3)}$ of Ag nanoparticles at the wavelength of the second harmonic radiation of a Ti:sapphire laser ($\lambda = 400$ nm) was measured to be 1.5×10^{-7} esu [3]. Ag nanoparticles have an advantage over other metal nanoparticles (i.e., Au and Cu) from the point of view that the SPR energy of Ag is far from the interband transition energy. So, in the Ag nanoparticle system, we can investigate the NLO processes caused solely by surface plasmon contribution.

In this direction, the NLO properties of Ag NPs embedded in SiO₂, TiO₂, and Al₂O₃ matrices have been reported [22, 23]. ZrO₂ has also emerged as an interesting choice of matrix because of higher refractive index, high band gap, and higher thermal stability as compared to other conventional oxide or polymer dielectrics [24, 25]. Anija et al. [26] have reported the NLO properties of different core–shell structures prepared by chemical route. However, to the best of our literature knowledge, the NLO properties of Ag:ZrO₂ NC thin films have not been investigated in detail so far. Such kind of study is very important because the stability of thin films (with nanometer thickness) to laser beam is usually considered a constraint during NLO measurements. Recently, we reported the synthesis procedure of Ag:ZrO₂ NC thin films without using any chemical capping agent and tailoring of SPR-induced absorption

with postdeposition treatments [27–29]. The present work mainly emphasizes on validating the role of Ag precursor concentration on the linear and nonlinear optical properties of NC thin films.

Fabrication and Experiment

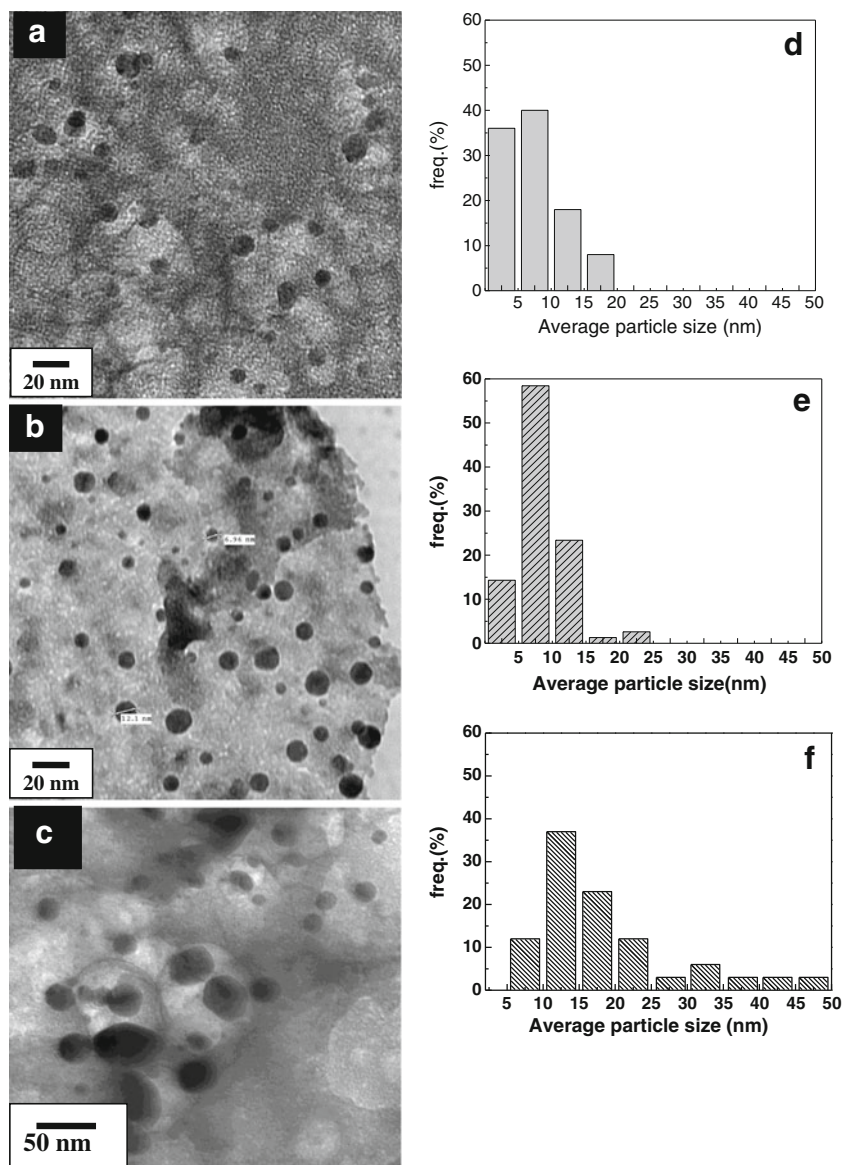
The Ag:ZrO₂ NC thin films (thickness ~ 300 nm) were prepared by sol–gel dip-coating method using different concentrations of Ag precursors (0.1, 0.05, and 0.025 M) followed by thermal annealing. The details of the synthesis methodology are described in our previous papers [27, 28]. Microstructural studies and Ag nanoparticle size estimation were carried out using a Philips TEM CM-12 fitted with a Hamamatsu digital camera model C-4742-95. The surface topography of films was recorded in contact mode with an atomic force microscope (Nanoscope IIIa Veeco). Optical measurements were recorded with a UV–VIS–NIR spectrophotometer (PerkinElmer, model: Lambda 900), and absorbance A ($A = 100 - R - T$) is calculated using the measured spectral transmittance (T) and spectral reflectance (R) data. To investigate the nonlinear optical properties of Ag:ZrO₂ NC films, an open-aperture z-scan measurement is carried out using 7-ns (FWHM) pulses from a Q-switched Nd:YAG laser (Quanta Ray Spectra Physics) emitting at the second harmonic wavelength at 532 nm (2.33 eV). A laser pulse energy of 15 μJ was used for the measurements.

Results and Discussions

TEM micrographs of the Ag:ZrO₂ NC films, prepared with 0.025, 0.05, and 0.1 M Ag precursor concentrations and annealed at 300 °C for 4 h are shown in Fig. 1 as a, b, and c, respectively. Micrographs show that grown Ag nanoparticles are spherical in shape and showing no agglomeration. Size (diameter) estimation shows that the size of the nanoparticles ranges mainly from 2 to 25 nm, and their distribution gets broadened with increase in Ag precursor concentration.

Particle size distributions of Ag NPs in films prepared with 0.025, 0.05, and 0.1 M Ag precursor concentration and identically annealed at 300 °C for 4 h are shown as d, e, and f, respectively, in Fig. 1. Histograms are plotted after estimating the size of 120 particles in each film. The distribution of particles is spread in the same range; however, the particle size shifts from 7 to 20 nm when the Ag concentration is increased. The average sizes of Ag particles are compared as a function of Ag precursor concentration, and it is observed that increase in Ag precursor concentration from 0.025 to 0.05 M, and to 0.1 M, results in growth of average size of the particles from 7 to 12 nm and to 20 nm, respectively (as shown in micrographs a, b, and c). A typical HRTEM micrograph of film annealed at 450 °C for 4 h (not shown here)

Fig. 1 TEM micrographs of Ag:ZrO₂ nanocomposite thin films, prepared with Ag conc. 0.025 M (a), 0.05 M (b), and 0.1 M (c), and corresponding size distribution of nanoparticles for Ag conc. 0.025 M (d), 0.05 M (e), and 0.1 M (f), annealed identically at 300 °C for 4 h

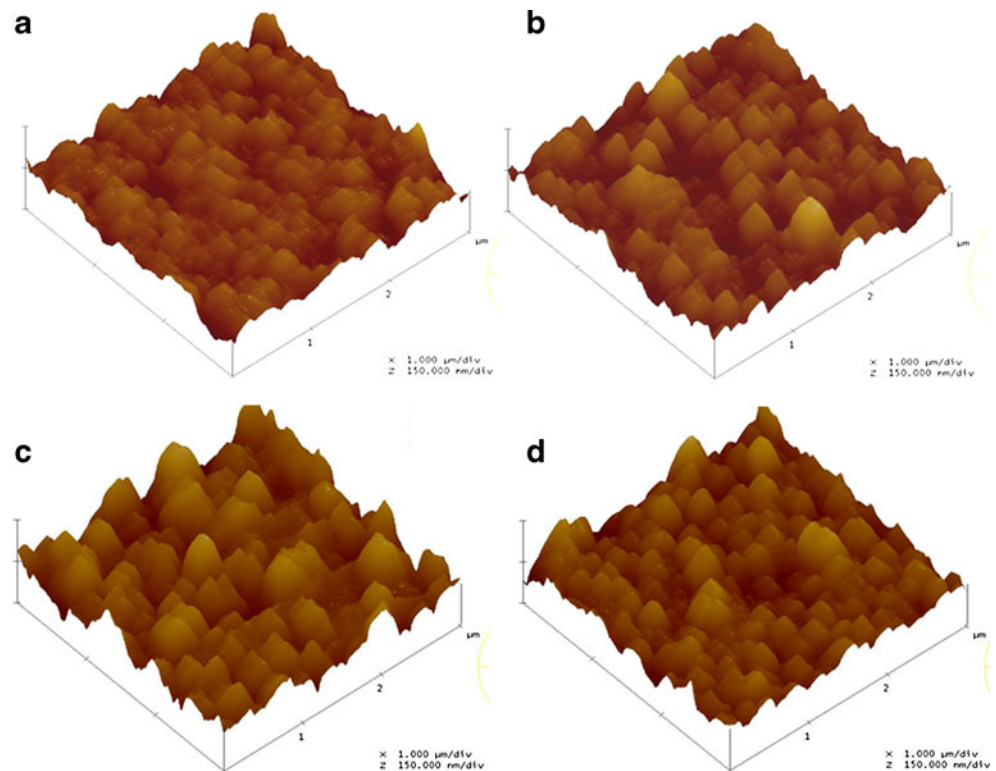


exhibits well-separated crystalline planes of Ag nanoparticles and of ZrO₂ matrix. The typical size of Ag nanoparticles in this case was found to be around 14 nm. If the average nanoparticle size is compared with Fig. 1 micrograph b, it is evident that the increase in the annealing temperature enhances the average nanoparticle size, which is in agreement with our earlier study [28].

Since the deposited films were prepared by sol-gel technique which involves sensitive variations in the porosity of films as a function of temperature, it may lead to a variation in surface features (i.e., roughness, areal density) which can have adverse effects in determining the linear and nonlinear optical properties of NC films. For this purpose, the surface topography of films is studied as a function of temperature. The surface topography of Ag:ZrO₂ NC films, *as deposited*, annealed for 4 h at 200, 300, and 450 °C, is shown by AFM

micrographs a, b, c, and d, respectively, in Fig. 2. These micrographs reveal that deposited films were dense, uniform, and intact on the substrate during thermal annealing; however, the surface topography exhibits significant variation. With the increase in annealing temperature from as deposited to 200 and to 300 °C, RMS roughness is found to increase from 16.4, to 26.7, and to 34.4 nm, respectively. However, a further increase in annealing temperature to 450 °C does not show an increase in RMS roughness and rather shows a decrease to 22.8 nm. The skewness variation is found to be -0.2, 0.5, 0.2, and 0.3 nm for films as deposited and annealed at 200, 300, and 450 °C, respectively. The reversal of negative values of skewness into positive values is evident from the fact that the as-deposited film has a porous surface structure, which gets modified, when films are annealed at temperature ≥ 200 °C. When the films were annealed up to 300 °C, the observed

Fig. 2 AFM micrographs of film as deposited (**a**), annealed at 200 °C (**b**), at 300 °C (**c**), and at 450 °C (**d**) [*x* and *y* scales, 1 μm per division, and *z* scale, 150 nm per division]



increase in RMS roughness from 16.4 to 34.4 nm is because in this temperature region, a remnant part of the solvent escapes, and conversion of silver oxide into Ag starts up. At 300 °C, the escaping is over, and further annealing to 450 °C does not increase RMS roughness, but a decrease is observed from 34.4 to 22.8 nm. Crystallization of the matrix at the same time leads to local rearrangement of metal clusters grown inside the porous ZrO₂ and hence modifies the surface roughness. If we compare the variation in RMS roughness of the NC films as a function of temperature with the incident spectral window of interest (around 400–600 nm), the variation is one order shorter than the incident wavelengths; hence, we can ignore the effects of surface variations in the present case.

Spectral variation in absorbance *A* versus incident light wavelength for the NC films prepared with different concentrations of Ag and annealed in identical conditions is shown in Fig. 3. The red and black curves correspond to the Ag concentrations of 0.025 and 0.05 M while blue traces correspond to 0.1 M. It is apparent from the figure that absorbance spectra exhibit resonance behavior depicting a strong absorption at a certain frequency of the incident light where incident light frequency matches with the natural frequency of oscillation of electrons in the particle which can be defined based upon the shape and size of the Ag nanoparticles. It can be noted from the figure that absorbance increases as the Ag concentration goes up. The absorbance is more prominent in the case of 0.1 M Ag concentration because of the largest size of the

nanoparticles compared with the cases of 0.05 and 0.025 M of Ag concentration. The observed red shift in peak position is also an indication of the growth of Ag nanoparticles with the increase in Ag precursor concentration.

In order to have an appreciation of the resonant absorbance behavior of metallic nanoparticles with respect to the incident radiation as well as shape and sizes of the nanoparticle, we theoretically analyzed our experimental observations. The optical response of noble metallic nanoparticles, embedded

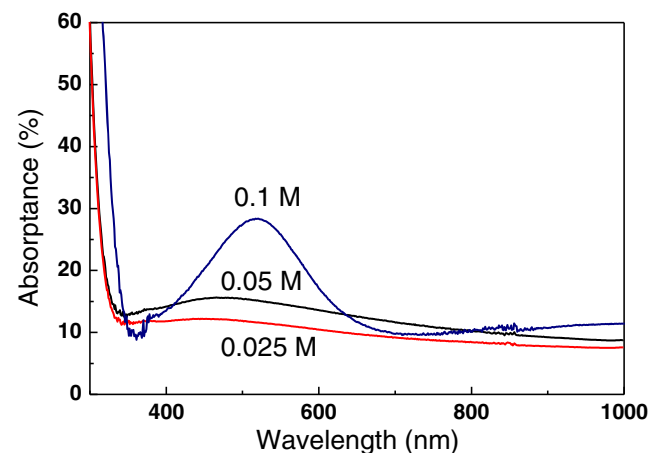


Fig. 3 Variation in SPR peak intensity, having fixed annealing conditions for Ag:ZrO₂ nanocomposite thin films of Ag concentrations of 0.025, 0.05, and 0.1 M

in a glass matrix, depends on size-dependent permittivity $\varepsilon(\omega, R)$ of Ag particles and absorption extinction (σ_{ext}) of Ag particles, as given in the following in the quasistatic regime where $R \ll \lambda$ [10]:

$$\varepsilon(\omega, r) = \varepsilon_1(\omega) + i\varepsilon_2(\omega, r) = \varepsilon_1(\omega) + i \left[\varepsilon_{2,\text{bulk}}(\omega) + \eta \frac{\omega_p^2}{\omega^3} \left(\frac{v_F}{r} \right) \right], \tag{1}$$

$$K = \frac{18\pi C \varepsilon_m^{3/2}(\omega) \varepsilon_2(\omega, r)}{\lambda \left((\varepsilon_1(\omega) + 2\varepsilon_m(\omega))^2 + \varepsilon_2^2(\omega, r) \right)} \tag{2}$$

where ε_1 and ε_2 are the real and imaginary parts of the dielectric constant of metal particles, ε_0 is the dielectric constant of the matrix, ω_p is the Drude plasma frequency (for Ag, $\omega_p = 1.46 \times 10^{16} \text{ s}^{-1}$), v_F is the Fermi velocity (for Ag, $v_F = 1.4 \times 10^6 \text{ ms}^{-1}$) and C is the volume concentration of embedded particles; the parameter η is written as the sum of two additive terms describing size and interface effects. From Eq. 2, it is evident that maxima in absorption extinction can be obtained if condition $\varepsilon_1(\omega) = -2\varepsilon_0$ is fulfilled, which leads to resonance when coupled with photons. This resonance corresponds to the first order mode of scattering of light by a metallic sphere. From Eqs. 1 and 2, it is clear that the position and the intensity of the absorption peak are strongly dependent on the size of particles and on the local environment.

In Fig. 4, we show the variation of SPR peak intensity with annealing duration of NC thin films prepared with two different Ag concentrations of 0.05 and 0.1 M at a fixed annealing temperature (300 °C). One may note that SPR peak intensity

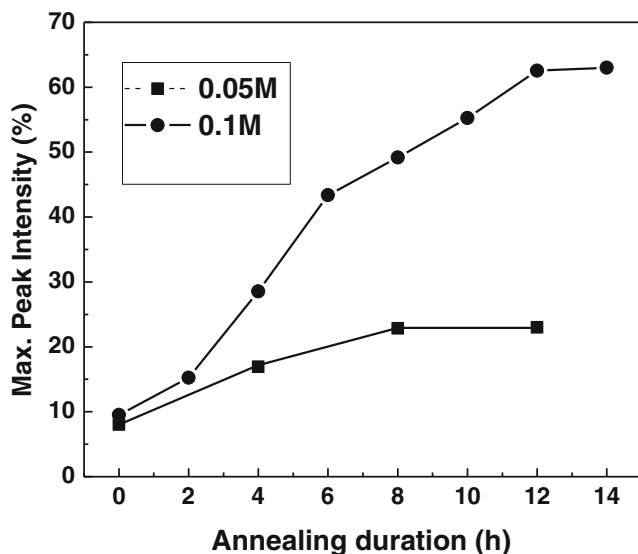


Fig. 4 Variation in SPR peak intensity, with different annealing durations for Ag:ZrO₂ nanocomposite thin films of Ag concentration of 0.05 and 0.1 M

initially increases with annealing duration and then saturates. The saturation times of 8 and 12 h are observed for the films prepared with 0.05 and 0.1 M Ag concentration, respectively. A rise in the peak intensity can be attributed to the continuum formation of Ag nanoparticles in the beginning when the yield of nanoparticles increases with time. Once the maximum nanoparticle concentration is achieved, the peak intensity is expected to saturate. The maximum nanoparticle concentration will occur when most of the Ag ions undergoing nucleation have been utilized in the formation of nanoparticles. Further, we observe that the rate of enhancement in peak intensity depends on the Ag concentration. A lower concentration of Ag nanoparticles, i.e., 0.05 M leads to a slower rate of formation and hence lesser time for saturation. This behavior is anticipated as the number of Ag ions is less in the lower Ag concentration film, leading to formation of less silver oxide molecules; hence, less thermal energy is needed for the decomposition of silver oxide into Ag nanoparticles. As evident from the figure, one may get the same absorbance A in less annealing duration for the higher Ag concentration.

The open-aperture z-scan technique has been used to measure the nonlinear optical properties. This technique is based on the single beam intensity versus transmission measurement, by focussing the beam and translating the sample in the focussed beam along the z-direction. We used a fully automated z-scan setup for the measurements [30]. The obtained open-aperture z-scan curves show the saturable absorption behavior. The observed NLO results can be modeled by using the homogenous equation describing saturation absorption [31]

$$\alpha(I) = \frac{\alpha_0}{1 + \left(\frac{I}{I_s} \right)} \tag{3}$$

Here, α_0 is the unsaturated linear absorption coefficient at the excitation wavelength, I is the input laser intensity, and I_s is the saturation intensity. For calculating the transmitted intensity for a given input intensity, the propagation equation,

$$\frac{dI}{dz'} = - \left(\alpha_0 / \left(1 + \frac{I}{I_s} \right) \right) I \tag{4}$$

is numerically solved. Here, z' indicates the propagation distance within the sample. By determining the best-fit curves for the experimental data, the nonlinear parameters are calculated.

Open-aperture z-scan curves of NC films prepared with Ag precursor concentrations 0.1, 0.05, and 0.025 M annealed at 300 °C for 4 h are shown in a, b, and c of Fig. 5, whereas the open-aperture z-scan curve of the NC film prepared with the

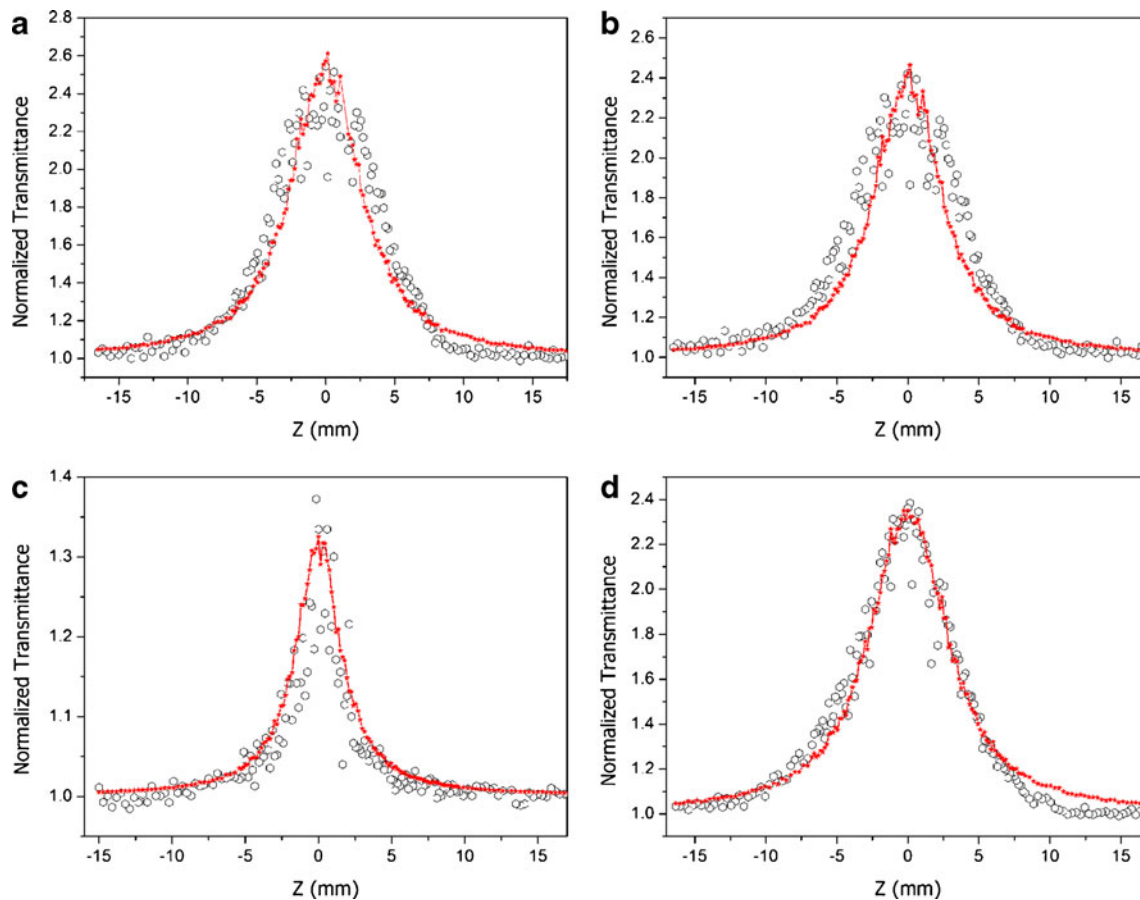


Fig. 5 Open-aperture z-scan curve of Ag:ZrO₂ nanocomposite films with Ag precursor concentration **a** 0.1 M, **b** 0.05 M, **c** 0.025 M (each annealed at 300 °C for 4 h), and **d** 0.05 M (annealed at 450 °C for 4 h)

Ag precursor concentration 0.05 M annealed at 450 °C for 4 h is shown in d. It has been observed that as-deposited films prepared with the highest Ag precursor concentration (0.1 M) were not stable at the highest laser fluence (i.e., at $z=0$). However, plots a, b, c, and d demonstrate that these NC thin films are stable with respect to highest fluence. For the quantitative evaluation of the saturation intensity (I_s), best-fit curves were obtained using Eqs. 3 and 4. Values of I_s are estimated as 1.3×10^{12} , 1.6×10^{12} , 6.1×10^{12} and 1.1×10^{12} W/m² for plots a, b, c, and d, respectively. The values of saturation intensities versus the estimated average sizes of Ag particle diameters are presented in Table 1. It is clear from the table that for

identical thermal conditions (300 °C for 4 h), the values of I_s increase with decrease in the average size of Ag nanoparticles. In the same line, when particle size was increased (from 12 to 14 nm) by increasing the annealing temperature (from 300 to 450 °C) for a fixed concentration of precursor (0.05 M), the decrease in values of I_s was induced. The contradicting trend in the case of films prepared with 0.1 M concentration annealed at 300 °C (average size=20 nm) and that of 0.05 M concentration annealed at 450 °C (average diameter=14 nm), where we observed a decrease in I_s , which can be explained considering the fact that the matrix of NC films, prepared with 0.1 M concentration and annealed at 300 °C, is mainly composed by Ag nanoparticles and matrix having Ag₂O₃ and ZrO₂, which affect the variation in the effective dielectric constants of matrix, and in turn on the nonlinear susceptibilities. Here, it must be emphasized that at annealing condition 300 °C for 4 h, we do not get the complete reduction of Ag₂O₃ into Ag, which is clearly evident from Fig. 4. The exact proportion of unreduced Ag₂O₃ can be estimated by comparing the core level spectra of silver oxide and of metallic Ag, which has already been elaborated in our earlier work [28]. On the other hand, in the matrix of NC films prepared with 0.05 M concentration and annealed at 450 °C, most of the

Table 1 The variation in saturation intensity versus the average particle size of Ag nanoparticles

No.	Ag precursor conc.	Annealing temperature	Particle diameter (avg.)	I_s (W/m ²)
1.	0.1 M	300 °C	20 nm	1.3×10^{12}
2.	0.05 M	300 °C	12 nm	1.6×10^{12}
3.	0.025 M	300 °C	7 nm	6.1×10^{12}
4.	0.05 M	450 °C	14 nm	1.1×10^{12}

Ag_2O_3 is decomposed in Ag metal, and the matrix is largely composed by ZrO_2 only. Such kind of complete decomposition of Ag_2O_3 into Ag at 450 °C has already been reported in our earlier work [28]. In the present case, the information is being obtained from the dependence of the detected signal on the position of sample with light induced lens along the focused laser beam. At resonance excitation, at least two contributions can take place; the first is the cumulative nonlinearity having a decay time much longer than the pulsewidth and associated with the population of excited states or local heating, and the second is Kerr nonlinearity having instantaneous response and decay times relative to the pulsewidth. Understanding the influence and strength of the individual contributions from an experimental or theoretical point of view would help to optimize materials. In order to improve saturable absorption, one has to understand the individual mechanisms that take place when intense laser light interacts with materials. Ganeev et al. reported the I_s values as $1.1 \times 10^9 \text{ W/cm}^2$ for Ag nanoparticles embedded in sodalime silicate glass and $1.4 \times 10^9 \text{ W/cm}^2$ for Ag nanoparticles embedded in silicate glass of 1-mm thickness [2]. In the comparison of such values, I_s in the present case (in the order of 10^{12} W/m^2) for ~300-nm-thick NC films will be an interesting choice of material for nanophotonic applications.

Conclusion

In conclusion, we have successfully synthesized Ag:ZrO₂ nanocomposite thin films and investigated their size-dependent linear and nonlinear optical properties in detail. The TEM micrographs of the nanocomposite films confirm the formation of spherical nanoparticles with diameters ranging from 7 to 20 nm by varying the Ag precursor and annealing conditions. The UV–VIS absorption studies revealed the existence of surface plasmon resonance absorption from Ag nanoparticles in the visible region. The intensity of the SPR peak was found to increase with Ag precursor concentration as well as with the annealing duration. The magnitude and sign of absorptive nonlinearities near the surface plasmon resonance of the Ag NPs in ZrO₂ matrix were measured by an open-aperture z-scan technique employing nanosecond-laser pulses. Z-scan results showed remarkable values of saturation intensities (in the order of 10^{12} W/m^2) for thin films which are found to be tunable with the varying Ag precursor concentrations as well as annealing temperature.

Acknowledgments One of the authors (M. Kumar) acknowledges the financial support as SRF given by the Council of Scientific and Industrial Research (CSIR), India, during this work. Authors also acknowledge the help received from Dr. Deepak Varandani for AFM imaging and Mr. V. K. Khanna for TEM imaging. YKM sincerely acknowledges the research fellowship from Alexander von Humboldt Foundation.

References

1. Plaksin O, Takeda Y, Amekura H, Kishimoto N, Plaksin S (2008) Saturation of nonlinear optical absorption of metal-nanoparticle composites. *J Appl Phys* 103:114302
2. Ganeev RA, Ryansnyansky AI, Stepanov AL, Usmanov T (2004) Saturated absorption and nonlinear refraction of silicate glasses doped with silver nanoparticles at 532 nm. *Op Quant Electron* 36:949–960
3. Inouye H, Tanaka K, Tanahashi I, Hattori T, Nakatsuka H (2000) Ultrafast optical switching in a silver nanoparticle system. *Jpn J Appl Phys* 39:5132
4. Anand PB, Sandeep CSS, Sridharan K, Narayanan TN, Thomas S, Philip R, Anantharaman MR (2012) An optical limiter based on silver-silica nanocomposites. *Adv Sci* 4:33–38
5. Unnikrishnan KP, Nampoorei VPN, Ramakrishnan V, Umadevi M, Vallabhan CPG (2003) Nonlinear optical absorption in silver nanosol. *J Phys D: Appl Phys* 36:1242–1245
6. Goncharenko AV, Chang YC (2007) Optical properties of core-shell particle composites. II. Nonlinear response. *Chem Phys Lett* 439: 121–126
7. Singh DB, Kumar G, Tripathi VK (2007) Nonlinear absorption of surface plasmons and emission of electrons from metallic targets. *Phys Plasmas* 14:102108
8. Bahae MS, Said AA, Wei T, Hagan DJ, Stryland EWV (1990) Sensitive measurement of optical nonlinearities using a single beam. *IEEE J Quantum Elect* 26:760
9. Battaglin G, Calvelli P, Cattaruzza E, Gonella F, Polloni R, Mattei G, Mazzoldi P (2001) Z-scan study on the nonlinear refractive index of copper nanocluster composite silica glass. *Appl Phys Lett* 78:3953–3955
10. Kreibig U, Vollmer M (1995) Optical properties of metal clusters. Springer, New York
11. Liu CS, Kumar G, Tripathi VK (2006) Laser mode conversion into a surface plasma wave in a metal coated optical fiber. *J Appl Phys* 100:013304
12. Kumar G, Tripathi VK (2007) Anomalous absorption of surface plasma wave by particles adsorbed on metal surface. *Appl Phys Lett* 91:161503
13. Plaksin O, Takeda Y, Amekura H, Kishimoto N (2006) Radiation-induced differential optical absorption of metal nanoparticles. *Appl Phys Lett* 88:201915
14. Zayats AV, Smolyaninov II, Maradudin AA (2005) Nano-optics of surface plasmon polaritons. *Phys Reports* 408:131–314
15. Kumar G, Singh DB, Tripathi VK (2006) Surface enhanced Raman scattering of a surface plasma wave. *J Phys D: Appl Phys* 39:4436–4439
16. Mishra YK, Adelung R, Kumar G, Elbahri M, Mohapatra S, Singhal R, Tripathi A, Avasthi DK (2013) Formation of self-organized silver nanocup-type structures and their plasmonic absorption. *Plasmonics* 8:811–815
17. Kumar M, Reddy GB (2010) Effect of atmospheric exposure on the growth of citrate capped Ag nanoparticles. *Physica E* 42: 1940–1943
18. Avasthi DK, Mishra YK, Kabiraj D, Lalla NP, Pivin JC (2007) Synthesis of metal–polymer nanocomposite for optical applications. *Nanotechnology* 18(12):125604
19. Mishra YK, Mohapatra S, Kabiraj D, Mohanta B, Lalla NP, Pivin JC, Avasthi DK (2007) Synthesis and characterization of Ag nanoparticles in silica matrix by atom beam sputtering. *Scr Mater* 56:629–632
20. Kreibig U (1970) Kramers Kronig analysis of the optical properties of small silver particles. *Z Physik* 234:307–318
21. Kreibig U (1974) Electronic properties of small silver particles: the optical constants and their temperature dependence. *J Phys F Metal Phy* 4:999–1014

22. Cesca T, Calvelli P, Battaglin G, Mazzoldi P, Mattei G (2012) Local-field enhancement effect on the nonlinear optical response of gold-silver nanoplanets. *Opt Express* 20:4537–4547
23. Mohapatra S, Mishra YK, Warriar AM, Philip R, Sahoo S, Arora AK, Avasthi DK (2012) Plasmonic, low-frequency Raman, and nonlinear optical-limiting studies in copper–silica nanocomposites. *Plasmonics* 7:25–31
24. Kumar M, Reddy GB (2011) Effect of sol-age on the surface and optical properties of sol–gel derived mesoporous zirconia thin films. *AIP Adv* 1:022111
25. Kumar M, Reddy GB (2008) A modified chemical route for synthesis of zirconia thin films having tunable porosity. *MRS Proc.* 1074E: 1074-I10-34
26. Anija M, Thomal J, Singh N, Nair AS, Tom RJ, Pradeep T, Philip R (2003) Nonlinear light transmission through oxide-protected Au and Ag nanoparticles: an investigation in the nanosecond domain. *Chem Phys Lett* 380:223
27. Kumar M, Kulriya PK, Pivin JC, Avasthi DK (2011) Evolution and tailoring of plasmonic properties in Ag:ZrO₂ nanocomposite films through swift heavy ions. *J Appl Phys* 109: 044311
28. Kumar M, Reddy GB (2009) Ag:ZrO₂ nanocomposite thin films derived using a novel sol–gel technique. *Phys Status Solidi B* 246: 2232–2237
29. Kumar M, Reddy GB (2010) Tailoring surface plasmon resonance in Ag:ZrO₂ nanocomposite thin films. *Physica E* 43:470–474
30. Suchand Sandeep CS, Philip R, Satheeshkumar R, Kumar V (2006) Sol–gel synthesis and nonlinear optical transmission in Zn_(1-x)Mg_xO ($x \leq 0.2$) thin films. *Appl Phys Lett* 89:063102
31. Seigman AE (1986) *Lasers*. University Science Books, Mill Valley